09_165.

 DOI 10.1002/pmic.200800848 *Proteomics* 2009, *9*, 3752–3764

RESEARCH ARTICLE

Proteome analysis demonstrates profound alterations in human dendritic cell nature by TX527, an analogue of vitamin D

Gabriela Bomfim Ferreira[1], Evelyne van Etten[1], Kasper Lage[2,3,4], Daniel Aaen Hansen[2], Yves Moreau[5], Christopher T. Workman[2], Mark Waer[6], Annemieke Verstuyf[1], Etienne Waelkens[7,8], Lut Overbergh[1] and Chantal Mathieu[1]

[1] Laboratory for Experimental Medicine and Endocrinology (LEGENDO), University Hospital Gasthuisberg, Catholic University of Leuven, Leuven, Belgium
[2] Center for Biological Sequence Analysis, Technical University of Denmark, Lyngby, Denmark
[3] Pediatric Surgical Research Laboratories, MassGeneral Hospital for Children, Massachusetts General Hospital, Boston, MA, USA
[4] Harvard Medical School, Boston, MA, USA
[5] ESAT–SDC, Department of Electrical Engineering, Catholic University of Leuven, Heverlee, Belgium
[6] Experimental Transplantation Section, University Hospital Gasthuisberg, Catholic University of Leuven, Leuven, Belgium
[7] ProMeta, University Hospital Gasthuisberg, Catholic University of Leuven, Leuven, Belgium
[8] Laboratory of Protein Phosphorylation and Proteomics, University Hospital Gasthuisberg, Catholic University of Leuven, Leuven, Belgium

Structural analogues of vitamin D have been put forward as therapeutic agents able to exploit the immunomodulatory effects of vitamin D, without its undesired calcemic side effects. We have demonstrated that TX527 affects dendritic cell (DC) maturation *in vitro*, resulting in the generation of a tolerogenic cell. In the present study, we aimed to explore the global protein changes induced by the analogue in immature DC (iDC) and mature human DC and to correlate them with alterations in DC morphology and function. Human $CD14^+$ monocytes were differentiated toward iDC or mature DCs, in the presence or absence of TX527 (10^{-8} M) ($n = 4$). Protein samples were separated into two different pH ranges (pH4–7 and 6–9), analyzed by 2-D DIGE and differentially expressed spots ($p<0.01$) were identified by MALDI-TOF/TOF (76.3 and 70.7% in iDC and mature DCs, respectively). Differential protein expression revealed three protein groups predominantly affected by TX527 treatment, namely proteins involved in cytoskeleton structure, in protein biosynthesis/proteolysis and in metabolism. Moreover, protein interactome-network analysis demonstrated close interaction between these different groups ($p<0.001$) and morphological and functional analyses confirmed the integrated effect of TX527 on human DCs, resulting in a cell with altered morphology, cell surface marker expression, endocytic and migratory capacity.

Received: October 30, 2008
Revised: March 27, 2009
Accepted: April 20, 2009



Keywords:
2-D DIGE / Dendritic cell / Immunotolerance / Network / Vitamin D analogue

Correspondence: Dr. Lut Overbergh, LEGENDO, UZ-Gasthuisberg, Onderwijs en Navorsing, Herestraat 49, bus 902, B-3000 Leuven, Belgium
E-mail: lut.overbergh@med.kuleuven.be
Fax: +32-16-34-60-35

Abbreviations: CCL, chemokine (C-C motif) ligand; **CCR,** chemokine (C-C motif) receptor; **DC,** dendritic cell; **GM-CSF,** granulocyte/macrophage colony-stimulating factor; **iDC,** immature DC; **IFN,** interferon; **IL,** interleukin; **mDC,** mature DC; **MFI,** mean fluorescence intensity

1 Introduction

The secosteroid hormone vitamin D_3, well known for its actions in bone and mineral homeostasis, has been rediscovered as a potential immunomodulator [1, 2]. Receptors for the active form of vitamin D ($1,25(OH)_2D_3$) are indeed present in most cells of the immune system and $1,25(OH)_2D_3$ can be produced by activated macrophages and

© 2009 WILEY-VCH Verlag GmbH & Co. KGaA, Weinheim

dendritic cells (DCs) [3–5]. *In vitro*, $1,25(OH)_2D_3$ alters the behavior of many immune cells, shifting T lymphocytes toward regulator cells and modulating monocyte cytokine profile, but the main target for $1,25(OH)_2D_3$ in a mixed immune cell population is the DC [6, 7], mainly the myeloid population [8]. Here, $1,25(OH)_2D_3$ induces a typical tolerogenic profile, with less antigen presentation and almost annihilation of interleukin (IL)-12 secretion [6, 9, 10]. Exploiting these interesting properties *in vivo* leads, however, to major issues of side effects, since the doses necessary for inducing these immune effects *in vivo* are well above the doses inducing life-threatening hypercalcemia.

To circumvent this issue, structural analogues of the molecule have been synthesized, sharing the immunomodulatory capacities, with less calcemic effects (or at least having a clearly dissociated effect) [11–13]. One such analogue is TX527, 19-nor-14,20-bisepi-23-yne-$1,25(OH)_2D_3$ [14]. This substance has been demonstrated to prevent diabetes in non-obese diabetic mice and to have the same immunomodulatory effects as $1,25(OH)_2D_3$, but at 100-times lower doses [15]. We have previously demonstrated that this analogue can dramatically alter the phenotype and the behavior of human DCs, resulting in a tolerogenic DC profile, affecting T-cell behavior in the absence of the analogue [7, 15].

The aim of the present study was to fully characterize the changes in DC protein profile, morphology and functionality induced by TX527 using an integrated approach, combining proteomics (2-D DIGE and MALDI-TOF/TOF), systems biology (interactome-network analysis) and functional studies. By this integrated approach we could demonstrate that TX527 initiates a complex process in human DCs, affecting proteins of different functional classes that interact closely together, finally resulting in a more tolerogenic DC-phenotype.

2 Materials and methods

2.1 *In vitro* generation of human DCs

Human peripheral blood mononuclear cells were isolated from four buffy coats of healthy donors by density gradient centrifugation (Lymphoprep, Axis-Shield, Oslo, Norway) and monocytes were purified subsequently by CD14-specific positive magnetic cell sorting according to the supplier's protocol (MACS, Milteny Biotec, Bergish Gladbach, Germany). Isolated monocytes ($\geq$90% pure, 1×10^6 cells/mL) were cultured in RPMI1640 medium (Gibco, Paisley, Scotland) supplemented with Glutamax-I (Gibco), 25 mM HEPES (Gibco), 5 μg/mL geneticin (Life Technologies, Rockville, MD, USA) and 10% heat-inactivated FCS(Gibco), in 75 cm^2 tissue culture flasks (TPP, Transadingen, Switzerland). For inducing DC differentiation, 1000 U/mL recombinant human IL-4 (Gentaur, Brussel, Belgium) and 800 U/mL granulocyte/macrophage colony-stimulating factor (GM-CSF) (Gentaur) were added. Medium and cytokines were refreshed on day 3. On day 6, immature DCs (iDC) were harvested for functional/morphological analysis and protein extraction, and maturation was induced in the remaining cultures, by addition of 100 ng/mL *Escherichia coli*-derived lipopolysaccharide (Sigma, St Louis, MO, USA), 1000 U/mL recombinant human interferon (IFN)-γ (Roche Diagnostics, Indianapolis, IN, USA) and 800 U/mL GM-CSF. Mature DCs (mDC) were harvested after an additional 48 h for functional/morphological analysis and protein extraction.

2.2 TX527 treatment of DCs

The analogue TX527 (19-nor-14,20-bisepi-23-yne-1,25 $(OH)_2D_3$)[14] was first synthesized by P. de Clerq and M. Vandewalle (Laboratory of Organic Chemistry, University of Ghent, Belgium) and further provided by J. C. Pascal and N. Adje (Merck-Theramex, Germany). It was used at a final concentration of 10^{-8} M, adding it every time the medium was refreshed.

2.3 2-D DIGE

Four independent cell culture experiments were carried out, each of them originating from a different healthy human blood donor. iDC and mDCs, treated or not with TX527 and obtained as described in Section 2.1, were washed with ice-cold PBS (Cambrex, Verviers, Belgium) and protein extraction followed by the 2-D DIGE experiments were carried out as previously described [16, 17]. Briefly, after extraction, protein content was determined with the Bradford method [18] and 50 μg of protein was labeled with 200 pmol of amine reactive cyanine dyes, Cy2, Cy3 or Cy5 (GE Healthcare) [16, 17, 19]. The pooled samples were loaded into individual 24 cm IPG strips, pH 4–7 and pH 6–9 and isoeletric focusing was carried out on an Ettan IPGphor II manifold (GE Healthcare) at 20°C for about 70 kV/h with a maximum current of 50 μA *per* strip. After isoelectric focusing, the IPG strips were equilibrated and run on a 1 mm thick 11.5% polyacrylamide SDS gel (25 × 20 × 0.5 cm; Ettan Dalt Six, GE Healthcare). The gels were run overnight at 20°C with a constant current of 8 mA/gel for 1 h, followed by 16 mA/gel until the end of the run. After the second dimension, the gels were scanned on a Typhoon 9400 gel imager (GE Healthcare) with 100 μm resolution and image analysis was performed using the Batch Processor module of the DeCyderTM V 6.5 software (GE Healthcare), following the manufacturer's recommendations.

Two preparative gels in each pH range for iDC and mDCs, treated or not with TX527, containing 350 μg of protein were run for spot picking. The gels were then post-stained with Krypton Staining (Thermo Fisher, Geel, Belgium) according to the manufacturer's protocol and the

© 2009 WILEY-VCH Verlag GmbH & Co. KGaA, Weinheim

spot matching was carried out on the BVA module of the DeCyder software. A pick list was generated and exported into the Spot Picker V1.20, the software that controls the Ettan Spot Picker (GE Healthcare). Spot manipulation was made as previously described [16, 17]. After digestion and extraction of the tryptic peptides, the peptide samples were concentrated and desalted with ZipTip C-18 (Millipore, Bedford, MA, USA) and analyzed by MS on a MALDI-TOF/TOF 4800 instrument (Applied Biosystems, Foster City, USA) as previously described [16, 17]. Data interpretation was carried out using the GPS Explorer software (Version 3.5), and database searching was carried out using the Mascot program (Version 2.2). Because all experiments were performed on human DCs, MS/MS searches were conducted with the following settings: MSDB (MS Protein Sequence Database) (taxonomy set on *Homo sapiens*, 148.148 protein entries) as database, MS/MS tolerance for precursor and fragment ions between 0.2 and 1 Da depending on the sample, methionine oxidation as variable modification and carbamidomethylation of cysteine as fixed modification. As enzyme, trypsin was selected, and a maximum of one missed cleavage was allowed. Using these parameters the probability-based Molecular Weight Search scores greater than the given cut-off value for MS/MS fragmentation data were taken as significant ($p<0.05$).

For all identified proteins, each sequenced peptide was individually aligned using BLAST [20]. For peptides matching different proteins, their SwissProt accession number is given. For peptides matching to different isoforms the following criteria were used for selecting which one to report. (i) If at least one of the identified peptides matched exclusively to a specific isoform or protein member, this protein isoform/member could be identified unambiguously. (ii) If all peptides matched one or more isoforms of the protein, the experimental molecular weight and p*I* obtained from the 2-DE gel was compared with the theoretical molecular weight and p*I* of the different isoforms/protein members. In case no single protein could be ruled out based on these criteria or possibly more than one member of the protein group could be present in a single spot, the different names/accession numbers are reported, including the percent identity between them (Supporting Information Tables 1 and 2).

2.4 Western blotting

Total protein extracts of iDC and mDCs, treated or not with TX527, from three different healthy donors were prepared as described in Section 2.3. Equal amounts (10 μg) of protein from each extract were solubilized in loading buffer (Invitrogen, Merelbeeke, Belgium) and subjected to SDS-PAGE (3–8 or 4–12% gradient gels, Invitrogen). Proteins were transferred to PVDF membranes, which were blocked (5% milk in PBS Tween 0.1%) for 1 h and then incubated with the following antibodies: mouse monoclonal anti-Fascin 1 (55K-2); rabbit polyclonal anti-Cathepsin S (H-50), both purchased from Santa Cruz Biotechnology, Santa Cruz, CA, USA; rabbit polyclonal anti-eEF2 (Cell signalling, Leiden, The Netherlands) and rabbit polyclonal anti-SOD2 (Upstate-Millipore, Brussels, Belgium). The membranes were then incubated with HRP-conjugated appropriated secondary antibody (anti-rabbit and anti-mouse, from Dako, Leuven, Belgium). Chemiluminescence was performed according to the manufacturer's instructions (PerkinElmer, Zaventem, Belgium). As a loading control, the membranes were re-probed with anti-GAPDH mouse monoclonal antibody (Applied Biosystems, Lennik, Belgium). Quantitative densitometry was carried out on the Typhoon 9400 gel imager (GE Healthcare). The detected bands were scanned with a 100 μm resolution and image analysis was performed using the 1-D gel analysis of ImageQuant software (GE Healthcare). The volume density of the chemiluminescent bands was calculated as the ratio between main antibody and loading control antibody after background correction.

2.5 Generating a human protein interaction network

Two human protein interaction networks were constructed as recently reported [21, 22]. Data were downloaded from BIND [23], MINT [24], IntAct [25], KEGG [26], Reactome [27], HPRD [28], DIP [28] and GRID [29]. In order to increase the coverage of interactions, interolog data (the transfer of protein interactions between orthologous protein pairs in different organisms) were included. Interactions were transferred from 17 eukaryotic organisms and added to the network. Orthology was assigned using the Inparanoid [30] orthology database using stringent thresholds. Each interaction was scored to assess its reliability by using a well-established scoring scheme [22, 31]. For each interaction the accumulated experimental proteomic evidence across all publications in the databases mentioned above was assessed. Furthermore, network topology surrounding the interaction was considered. This measure favors interactions between proteins with many common interaction partners, which is a well-established measure of the reliability of the interaction. These two parameters were merged and an overall confidence score was assigned to the interaction. The optimal cut-off separating signal from noise was determined by optimizing against a set of expert curated human protein interactions.

2.6 Constructing the networks and determining their significance

The network in Fig. 2A was constructed by expanding in the first order from TX527-treated iDCs (A) and determining all first-order interaction partners, we call these linker proteins. Then linker protein was scored based on its interaction propensity to the input set described in detail in [16, 32]. The scores on the interaction partners were incrementally tested

© 2009 WILEY-VCH Verlag GmbH & Co. KGaA, Weinheim

and for each propensity score network significance was calculated. The propensity score that gave the most significant network (see below) was chosen and the network was constructed including only linker proteins scoring above this propensity score, to ensure networks with the highest possible biological signal. The network in Fig. 2B was constructed analogous to the described procedure.

2.7 Determining the significance of an interaction network

The reported significances of the networks were determined by comparison with the enrichment of input proteins in a given network compared with enrichment of random sets of proteins in networks generated by the same method as described in detail in [16, 32]. Specifically, for an input set of N input proteins yielding an interaction network (connected component) with G input proteins and T total proteins a network score (NS input) was determined. This network score is the fraction of input proteins of all proteins in the network (G/T). We then determined the significance of the network score by empirically estimating the probability of observing a similar or better network score in networks generated by using 10 000 random input sets of size N input. The random gene sets were chosen so that the degree distributions of proteins in the random sets approximate the input set. As each query generates a varying number of networks (connected components), the probability estimates can be calculated from the total amount of networks produced by all 10 000 randomizations that have a network score > NS input. For this reason network *p*-values can be lower than the amount of random queries.

2.8 Phenotypic analysis of human DCs

2.8.1 Analysis of DC surface markers

For analysis of DC surface markers, 2.5×10^5 DCs were incubated for 30 min at 4°C with the following FITC- or PE-conjugated human antibodies: CD1a, CD14, CD80, CD40 (all from eBiosciences, San Diego, CA, USA); HLA-DR, CD83, CD86, chemokine (C-C motif) receptor (CCR)5, CCR7 (all from Becton Dickinson, San Jose, CA, USA) and corresponding control antibodies, all diluted in PBS. After washing and fixing in 1% paraformaldehyde, the cells were analyzed on a FACSsort (Becton Dickinson). Expressed data were corrected for control antibodies. fluorescent-activated cell sorting analysis was performed on DCs from three different donors.

2.8.2 Chemotaxis assay

Active migration toward chemokine (C-C motif) ligand (CCL) 3 and CCL19 was evaluated by a transwell assay. Briefly, lower chambers of polycarbonate membrane Transwell plates (6.5 mm-diameter, 5.0 μm-pore size, Corning, New York, USA) were filled with 600 μL complete medium containing 100 ng/mL recombinant human MIP1-α/CCL3 or MIP-3-β/CCL19 (Peprotech, UK). A control condition, without chemokines, was included. Control and TX527-treated mDCs (2.5×10^6 cells) were added to the upper chambers in 100 μL complete medium. Cells were allowed to migrate for 2 h at 37°C. The percentage of migrating cells was calculated as a ratio between the number of migrating cells and the initial number of cells. Specific migration was calculated by subtracting the mean number of spontaneously migrating cells (migration to medium only) from the mean number of cells that migrated in response to the chemokine.

2.8.3 Endocytosis assay

iDCs (2×10^5 cells) treated or not with TX527 were pre-cooled at 4°C for 30 min and then incubated at 37°C for 90 min with either FITC–dextran (1 mg/mL, Sigma), for the analysis of mannose receptor-mediated endocytosis, or Lucifer Yellow (1 mg/mL, Sigma), for the evaluation of fluid-phase endocytosis. As a negative control, cells were incubated with either one of the reagents at 4°C for 90 min. Cells were washed three times in ice-cold PBS supplemented with 1% FCS, fixed in ice-cold 1% paraformaldehyde and immediately analyzed by fluorescent-activated cell sorting. Specific endocytosis was calculated by subtracting the mean fluorescence intensity (MFI) of endocytosed cells at 4°C from the percentage of endocytosed cells at 37°C.

2.8.4 Immunofluorescence staining

iDC and mDCs, treated or not with TX527 (2×10^5 cells), were allowed to adhere on 1.2 cm diameter cover slips treated with Cel-tak 3 μg/cm^2 (Becton Dickinson) at RT for 1 h. Cover slips were rinsed with PBS and cells were fixed in 4% formalin for 15 min. After rinsing again in PBS, cells were permeabilized for 15 min with PBST (0.5% Triton X100), which was removed and block buffer (0.4% fish skin gelatin in PBS) was added for 30 min. Mouse monoclonal anti-Fascin 1 (55K-2) (Santa Cruz Biotechnology) antibody diluted (1:250) in PBS with 0.2% Triton X100 and 1% BSA was added to the cover slips and incubated overnight at 4°C. The following day, primary antibody was removed, cover slips were rinsed with PBS Tween (0.5% Tween-20) and secondary fluorescent-labeled antibody (Alexa Fluor 633 goat anti-mouse IgG, Invitrogen) was diluted (1:5000) in blocking buffer, together with 12.5 μL/mL of rhodamine phalloidin antibody (Invitrogen) and incubated at 37°C for 1 h. Cover slips were rinsed with PBS and mounted on the top of SuperFrost slides (Fisher Bioblock Scientific, Illkirch, France) with three drops/cover slip of ProLong Gold mounting media (Invitrogen).

© 2009 WILEY-VCH Verlag GmbH & Co. KGaA, Weinheim

2.9 Statistical analysis

The statistical differences between group average ratios were determined by unpaired two-tailed Student's *t*-Test, performed automatically by the BVA module of the DeCyder V6.5. $p<0.01$ was considered statistically significant. For the functional/morphological assays, statistical tests performed were two-tailed Student's *t*-Test and $p<0.05$ was considered statistically significant.

3 Results

3.1 TX527-induced protein profile of human DCs: 2-D DIGE and protein identification

Human $CD14^+$ monocytes were isolated from peripheral blood mononuclear cells of healthy donors. These were differentiated towards iDCs (6 days in the presence of IL-4 and GM-CSF) and in addition maturated into mDCs (two additional days in the presence of GM-CSF, lipopolysaccharide and IFN-γ) in the presence or absence of TX527 (10^{-8} M) during the whole culturing period. The high purity of the obtained DCs and reproducibility of the cultures were verified by flow cytometric analysis of classical DC surface markers. Treatment with TX527 induced changes on the DC surface phenotype, giving rise to cells that are $CD14^+$ and have reduced expression of co-stimulatory molecules (CD40, CD80 and CD86), as well as CD1a, CD83 and MHCII (Supporting Information Fig. 1).

In iDCs, 1857 ± 20 spots were matched on the pH 4–7 range and 1592 ± 69 spots on the pH 6–9 range. From these, 118 spots (85 up-regulated, 33 down-regulated) were differentially expressed in the DC exposed to TX527 treatment (TX-iDC, $p<0.01$) and for 90 of these spots (76.3%, 44 distinct proteins) the exact nature of the protein could be determined by MALDI-TOF/TOF (Supporting Information Fig. 2A). In mDCs, 1755 ± 70 spots could be matched between all donors and all conditions for pH 4–7 and 1634 ± 76 spots for pH 6–9, 140 of which (99 up-regulated, 41 down-regulated) were differentially expressed in DCs exposed to TX527 (TX-mDC, $p<0.01$). Protein identification was successful for 99 of the differentially expressed spots (70.7%, 63 distinct proteins) (Supporting Information Fig. 2B). The complete list of identified proteins is shown in Supporting Information Tables 1 and 2.

Gene ontology classification showed that the identified proteins could be divided into different functional groups, as described in Supporting Information Tables 1 and 2. The majority of proteins affected by TX527 treatment, in iDCs as well as in mDCs, could be classified in the categories of metabolic proteins, cytoskeleton proteins and proteins involved in protein biosynthesis/proteolysis.

Most of the metabolic proteins are up-regulated by the treatment, with some being present in multiple forms pointing to the possible occurrence of post-translational modifications, *i.e.* phosphorylation, glycosylation or even proteolytic cleavage. Carbonic anhydrase, for instance, is present in 15 and 11 different forms in iDCs and mDCs, respectively, all being induced at very high levels (between 1.66 and 9.71-fold, $p<0.001$). Another protein present in multiple forms is fructose-1,6-bisphosphatase, being altered in 16 and 6 different forms in iDCs and mDCs, respectively (between 1.79 and 4.66-fold, $p<0.001$).

Most of the cytoskeleton proteins are down-regulated by TX527 treatment, such as fascin (two and three spots down-regulated in TX527-treated iDC and mDC, compared with respective non-treated controls, $p<0.01$) and lymphocyte-specific protein 1 (two and four spots all down-regulated, respectively, in TX527-treated iDC and mDC, $p<0.01$). The only protein that was highly up-regulated in this functional group, was vimentin (between 1.88 and 4.74-fold induced in five separate spots in TX-mDCs, compared with their non-treated controls, $p<0.01$).

Another highly represented group of proteins altered by TX527 treatment are those involved in protein biosynthesis and proteolysis. Here, the main group of proteins altered by TX527 in iDCs play a role in translation, such as elongation factor 1-γ (eEF1G), elongation factor 2 (eEF2), elongation factor Tu (eEFTu), protein-glutamine γ-glutamytransferase 2 (PGGT2), eukaryotic translation initiation factor 3 subunit 3 (EIF3S3) and eukaryotic translation initiation factor 4H (EIF4H); all of them being significantly up-regulated ($p<0.01$). In TX527-treated mDCs the most affected proteins in this group are involved in the MHCI/II pathway, *i.e.* cathepsin D (CTSD) (more then two-fold induced in three different spots, $p<0.01$), cathepsin S (CTSS) (2.57-fold induced, $p<0.01$), cytosol aminopeptidase (LAP3) (1.43-fold decreased, $p<0.01$) and proteasome activator complex subunit 2 (PA28-β) (2.18-fold decreased, $p<0.01$), were mainly affected.

Moreover, spot identification revealed moreover interesting proteins affected by TX527 treatment in less represented functional groups. For example, in TX-treated mDCs, a number of proteins involved in the stress response were clearly up-regulated, such as 150 kDa oxygen-regulated protein (ORP150), chaperonin GroEL (precursor) (HSPD1) mortalin, and thioredoxin domain-containing protein 4 (TXNDC4), whereas others were down-regulated (105 kDa – HSPH1 and serine/threonine-protein phosphatase 2A – PPP2R1A). Four annexins (ANXAI, II, V and VI) were differentially expressed either in iDC or mDCs, two of which having the same regulation in both TX-treated iDC and mDC (ANXAII, up-regulated; ANXAVI, down-regulated). Furthermore, leukotriene A-4 hydrolase (LTB4) and neutrophil cytosol factor 2 (p67phox), proteins involved in the cellular defense response, are up-regulated by TX527 in mDCs. Finally, the protein swiprosin 1, which has only been described in lipid rafts in B cells [33] and $CD8^+$ T lymphocytes [34], was down-regulated both in TX-iDCs and TX-mDCs.

© 2009 WILEY-VCH Verlag GmbH & Co. KGaA, Weinheim

3.2 TX527-induced protein profile of human DCs: Western blotting

In order to validate the data obtained from 2-D DIGE, Western blot analysis was performed for four key proteins abundantly expressed and clearly altered by TX527 either in iDCs or in mDCs. Proteins that were chosen were involved in different cellular processes, *i.e.* fascin, a cytoskeleton protein which is down-regulated in TX-iDCs and TX-mDCs; CTSS, which degrades the invariant chain in MHCII molecules, found to be up-regulated in TX-mDCs; eEF2, involved in protein elongation and up-regulated in TX-iDCs; and finally SOD2, a stress response protein, found in three up-regulated spots in TX-mDCs.

Western blot analysis confirmed the differential expression pattern for all of these proteins (fascin 9.1 ± 0.15-fold

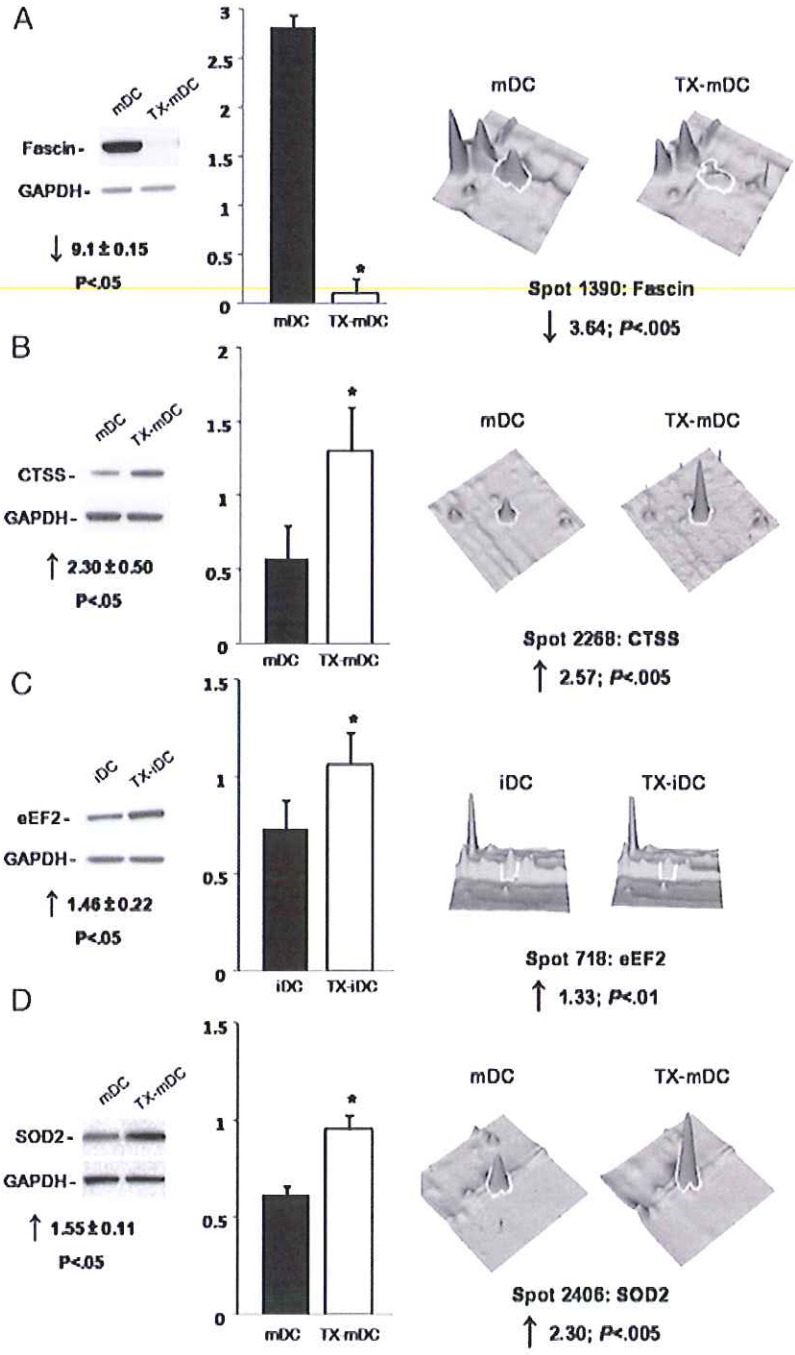


Figure 1. Protein expression levels of Fascin, CTSS, eEF2 and SOD2. iDC and human mDCs treated or not with TX527 (10^{-8} M) were lysed and the protein levels were analyzed by Western blotting with appropriate specific antibodies: (A) Fascin, (B) CTSS, (C) eEF2 and (D) SOD2. As loading control, the membranes were re-probed with anti-GAPDH antibody. The immunoblots shown are representative of a total of three independent experiments. The corresponding histograms show the relative increase of all normalized densitometric values, $^{*}p<0.05$. The results are presented as the (mean ± SD) of three independent experiments. The graphs seen on the right-hand side of the histograms are representative 3-D views of the bidimensional gel area where the correspondent spots for the four confirmed proteins are localized, together with their spot number, fold-induction and *p*-value assessed by the 2-D DIGE technique.

© 2009 WILEY-VCH Verlag GmbH & Co. KGaA, Weinheim

decreased in TX-mDCs, $p<0.05$; CTSS 2.30 ± 0.50-fold increased in TX-mDC, $p<0.05$; eEF2 1.46 ± 0.22-fold increased in TX-iDC, $p<0.05$; and SOD2 1.55 ± 0.11-fold increased in mDC, $p<0.05$) (Fig. 1).

3.3 Interactome-network analysis

To investigate whether the differentially expressed proteins are part of an integrated interactome, the identified proteins were placed in two distinct protein interaction networks – one for iDCs and one for mDCs – making use of a sophisticated network program recently developed [21, 22].

This analysis revealed that 28 out of the 44 proteins altered by TX527 in iDCs are tightly linked ($p<0.001$). As demonstrated in Fig. 2A, all proteins involved in protein biosynthesis and proteolysis – mainly representing proteins involved in initiating and elongation of translation – are represented in this network, suggesting a central effect of TX527 on this pathway in iDCs. These altered proteins seem to interact closely with proteins from other functional groups, including cytoskeleton, metabolism, apoptosis, calcium binding and electron transport.

In mDCs the network picture is more complex, with 41 out of the 64 proteins altered by TX527 being tightly linked ($p<0.001$). Here, the majority of proteins involved in metabolism, protein biosynthesis/proteolysis and cytoskeleton organization are represented in the network (Fig. 2B). This suggests that the proteins do not work as single entities, but rather as an integrated interactome, linking proteins from different functional classes.

3.4 TX527-induced DC phenotype: Functional implications of alterations in cytoskeleton proteins

3.4.1 Alterations in morphology and cytoskeleton

Control iDCs are round-shaped cells in suspension, with cytoplasmic protrusions that become more evidenced in mDCs (Figs. 3A and B). Upon TX527 treatment the cytoplasmic protrusions disappear and the cells become adherent and spindle-shaped, evident both in iDCs and mDCs (Figs. 3C and D).

Immunofluorescence microscopy on the intracellular localization of two cytoskeleton key proteins, fascin and actin, revealed altered distribution of these proteins in TX527-treated DCs. As shown in Figs. 3E and F, control DCs, both immature and mature, are round shaped, with filamentous actin and fascin co-localizing and primarily residing at the plasma membrane. Upon TX527 treatment, the distribution of both fascin and actin is more scattered throughout the cell, both in iDC and mDCs (Figs. 3G and H).

3.4.2 Alterations in migratory and endocytic capacity

As cytoskeleton plays a major role in DC motility, we evaluated the migratory capacity of TX527-treated DCs *versus* untreated DCs. We studied migration in response to chemokines and chemical stimuli.

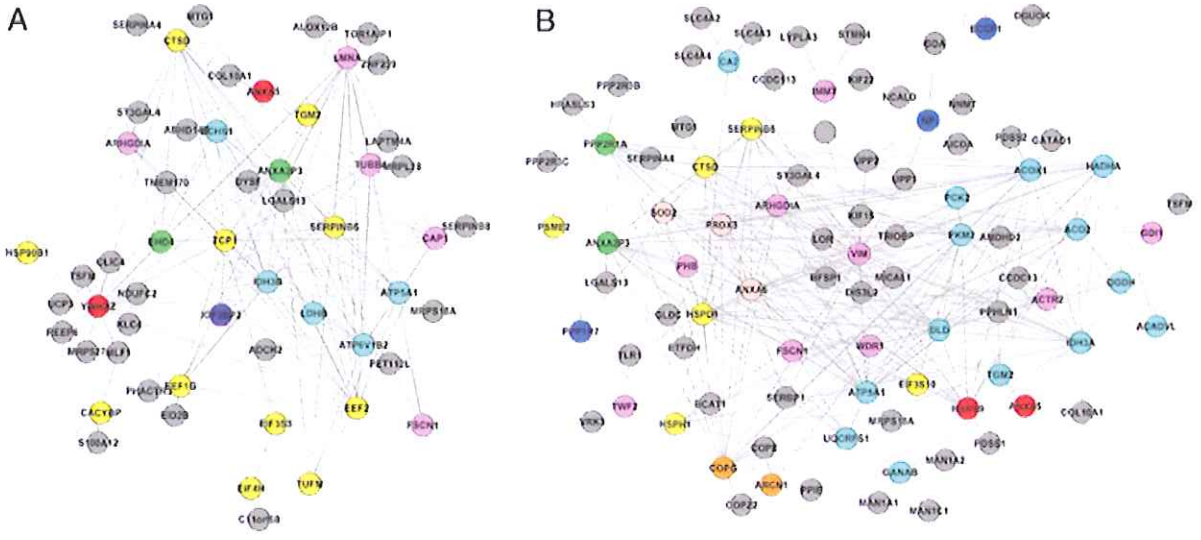


Figure 2. Protein interaction networks A protein interaction network, revealing that 28 out of 44 different proteins identified in TX527-treated iDCs (A) and 41 out of 64 proteins identified in TX527-treated mDCs (B) identified in this study constitute a significant interaction ($p<0.001$). Colored circles represent proteins identified in this study, while gray circles correspond to interconnecting proteins identified by the software program. The colored proteins are divided in functional groups as follows: metabolism (light blue), signal transduction (green), cytoskeleton-related proteins (pink), protein biosynthesis/proteolysis (yellow), transport (orange); DNA replication and modification/RNA binding protein (dark blue); response to oxidative stress/cellular defense response (light pink); anti-apoptosis (red). For full names of abbreviations, see Supporting Information Table 1.

© 2009 WILEY-VCH Verlag GmbH & Co. KGaA, Weinheim

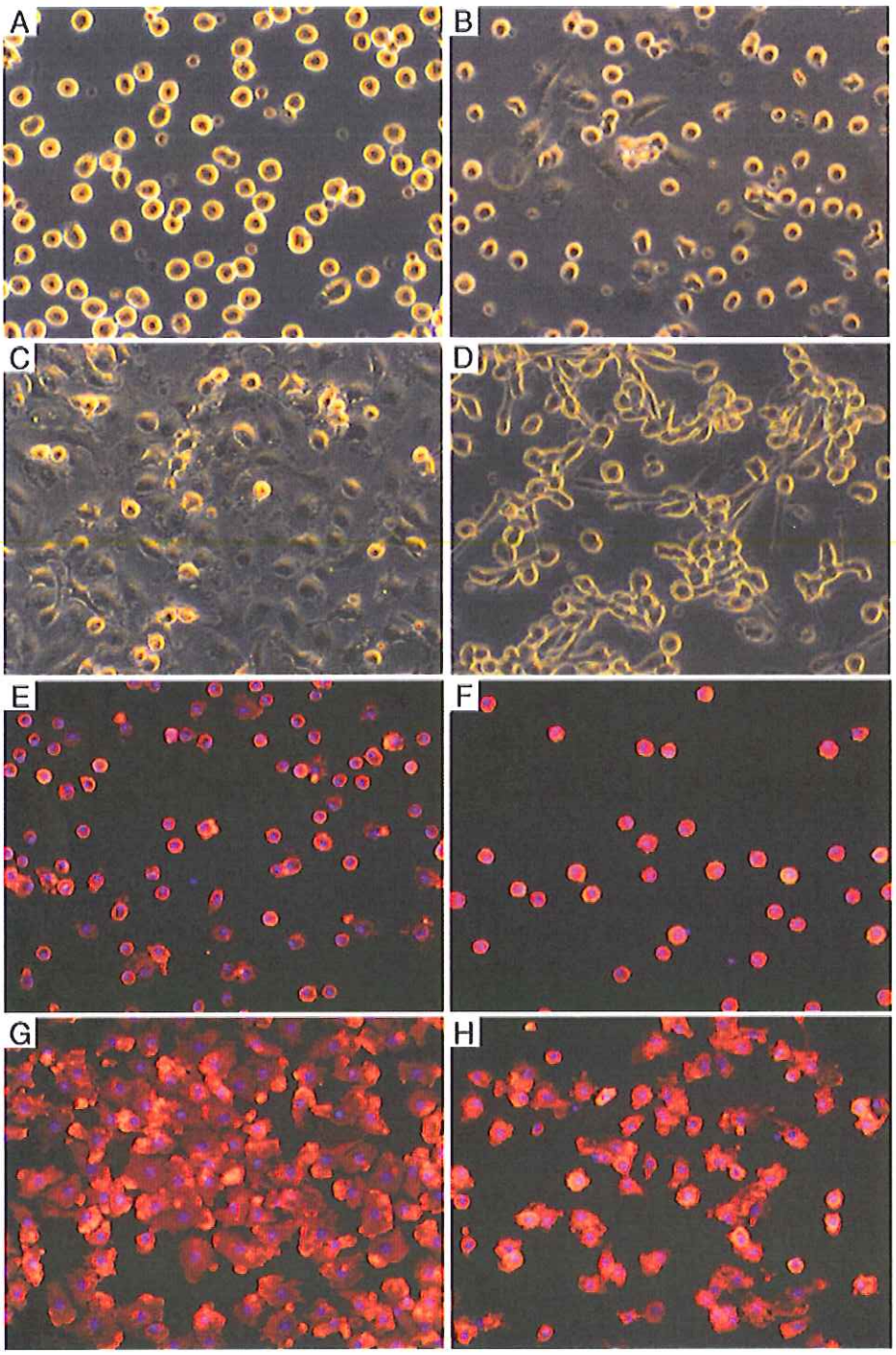


Figure 3. TX527 alters morphology and actin/fascin localization in human DCs. (A–D) Morphology of human DCs. The pictures are representative of a total of four independent experiments corresponding to control iDCs (A), control mDCs (B), TX527-treated iDCs (C) and TX527-treated mDCs (D). (E-H) Immunofluorescence of human DCs stained with filamentous actin (yellow) and fascin (pink) fluorescent antibodies. Pictures show overlay images obtained from (E) control iDCs (E), control mDCs (F), TX527-treated iDCs (G), and TX527-treated mDCs (H). One out of three independent experiments is shown.

Migration induced by the chemokines MIP1-α/CCL3 and MIP3-β/CCL19 was clearly influenced by TX527 treatment. Indeed, TX-mDCs migrated significantly less toward the CCR7-ligand, CCL19 (23% in control mDCs *versus* 4.9% in TX-treated mDC, $p<0.01$), whereas migration toward the CCR5-ligand, CCL3, was significantly increased (0.5% in control mDCs *versus* 4.4% in TX-treated mDCs, $p<0.05$). This altered migratory capacity fully correlated with changes in mDC surface receptor expression, with increased expression of CCR5 (background MFI in control mDC *versus* MFI of 27.61 in TX-mDCs) and decreased expression of CCR7 (MFI 13.2 in control mDC *versus* background MFI in TX-mDCs).

© 2009 WILEY-VCH Verlag GmbH & Co. KGaA, Weinheim

To investigate migratory and endocytic capacity at once, iDCs were exposed to fluid (Lucifer yellow) and solid (FITC-dextran) antigen. Migration toward and endocytosis of fluid antigen was almost completely blocked by TX527 treatment (3.93 ± 0.14-fold inhibition in TX-iDCs *versus* control iDCs, $p<0.05$), whereas solid endocytosis (FITC-dextran) was unaffected (1.21 ± 0.25-fold in TX-iDCs *versus* control iDCs, p NS).

4 Discussion

$1,25(OH)_2D_3$ is a major modulator of the immune system, mainly because of its direct effects on DCs. By affecting DC differentiation and maturation [6,10], $1,25(OH)_2D_3$ induces tolerogenic DCs *in vitro* and *in vivo*, with major changes in DC morphology, surface phenotype and activation state. Indeed, we and others have described that surface expression of MHCII, costimulatory molecules (CD80, CD86, CD40) and other maturation molecules (CD1a and CD83) are importantly down-regulated during maturation of DCs in the presence of $1,25(OH)_2D_3$, leading to a profound modulation of their antigen presenting and T-cell stimulatory capacity [7, 35].

The structural analog of vitamin D, TX527, has been put forward by our group as a potential tool for affecting the immune system *in vivo*, since it shares with $1,25(OH)_2D_3$ immunomodulatory properties, but has less calcemic effects. We have demonstrated that TX527 does not simply abrogate differentiation and maturation of DCs but rather leads to the emergence of a different cell type that lacks typical DC features. In the present study, a global proteomic 2-D DIGE approach coupled with interactome-network analysis allowed us to demonstrate that TX527 affects the human DC in a dramatic way, altering several protein pathways in different levels.

Proteins involved in cytoskeleton turnover, cell migration, cell growth and vesicle movement were mainly down-regulated, with a clear reflection in DC morphology, with shorter and less dendrites and especially a disturbed filamentous actin and fascin network under the plasma membrane. Fascin is known to be highly expressed during the maturation process, playing an important role in cytoskeleton remodeling [36], a process counteracted by TX527, resulting in a major decrease of different forms of fascin. Since fascin has a role in the assembly of dendritic protrusions, DC migration and T-cell activation [37–39], as well as in the formation of stable F-actin bundles, which are essential for the stability of the cell membrane and membrane-dependent processes, such as migration, motility, phagocytosis and division [40–42], the observed decrease in fascin will again add to the altered DC morphology. Indeed, these changes may diminish the establishment of DC–T-cell contacts, deteriorate DC–T-cell interaction and decrease secretion of cytokines by T cells [37, 43].

Not only actin and fascin, but also a number of other cytoskeleton-related proteins were altered by TX527. Actin-like protein 2 and actin interacting protein 1 (AIP1), for instance, are part of the Arp2/3 protein complex, which is a major mediator of actin polymerization that nucleates branching networks of F-actin [44]. The knock-down of AIP1 in LAK/T-cells has been shown to give rise to flattened cells [45]. Rho GDP-dissociation inhibitor 1 (RhoGDI), also down-regulated by TX527, plays a central role in cytoskeletal dynamics, adhesion and motility [46], whereas lymphocyte-specific protein 1, normally up-regulated during DC maturation [47], but down-regulated by TX527, participates in at least two cytoskeleton-dependent phenomena, namely phagocytosis/vesicle trafficking in iDCs and migration/motility in mDCs.

Interestingly, by using chemokines as stimulators of migration, we discovered that TX527 treatment did not fully paralyze the DC, since response to CCL3 gradients was enhanced by TX527. Indeed, when studying migration in response to chemokines, not only cytoskeleton, but also the presence of chemokine receptors plays a role. The group of Gauzzi [48] have previously demonstrated that $1,25(OH)_2D_3$ disrupts the ability of type I IFN-generated DCs to migrate in response to inflammatory and lymph-node homing chemokines. Here we show a differential effect of TX527 treatment on DC migration, dependent on regulation of chemokine receptor expression and cytoskeleton alterations, again confirming that treatment of DCs with vitamin D analogs not just blocks differentiation or maturation, but results in a fully different cell-type, with altered chemokine-receptor expression and migration activity. This conclusion is supported by the observation that endocytosis by TX527-treated DCs of fluid antigen was severely affected, but that of solid FITC-dextran antigen was not.

Metabolic proteins were also found to be profoundly altered by TX527. In this group, these proteins were included in a pathway indicating that the β-oxidation metabolism and Krebs cycle are increased by TX527 treatment in mDCs (Fig. 4). Interestingly, a recent report [49] indicated that PPAR-γ receptor ligands have the ability to primarily induce the expression of lipid/fatty acid metabolism genes in human DCs, to down-regulate some of their surface molecules, such as CD1a, CD80/86 ratio, CD83, CD40 and CCR7 and to decrease IL12p70, CXCL10 and RANTES secretion, thus acting similarly as the VDR-ligand, $1,25(OH)_2D_3$. In addition, a rising theme in the research on the mechanism of action of $1,25(OH)_2D_3$ includes the study of the effects of this hormone on PPAR-γ activation. Indeed, $1,25(OH)_2D_3$ treatment has been shown to induce PPAR-γ expression in primary human keratinocytes [50]. However, the role of lipid metabolism in DCs remains to be elucidated. The up-regulation of the β-oxidation pathway in mDCs increases the production of reactive oxygen species by the electron transport chain in the mithochondria, increasing the expression of anti-oxidative proteins, such as peroxiredoxin 3 (Prx3, 1.54-fold increased in TX527-treated mDCs) and superoxide dismutase (SOD2; three spots increased in TX527-treated mDCs). SOD2 has previously been shown to be up-regulated

© 2009 WILEY-VCH Verlag GmbH & Co. KGaA, Weinheim

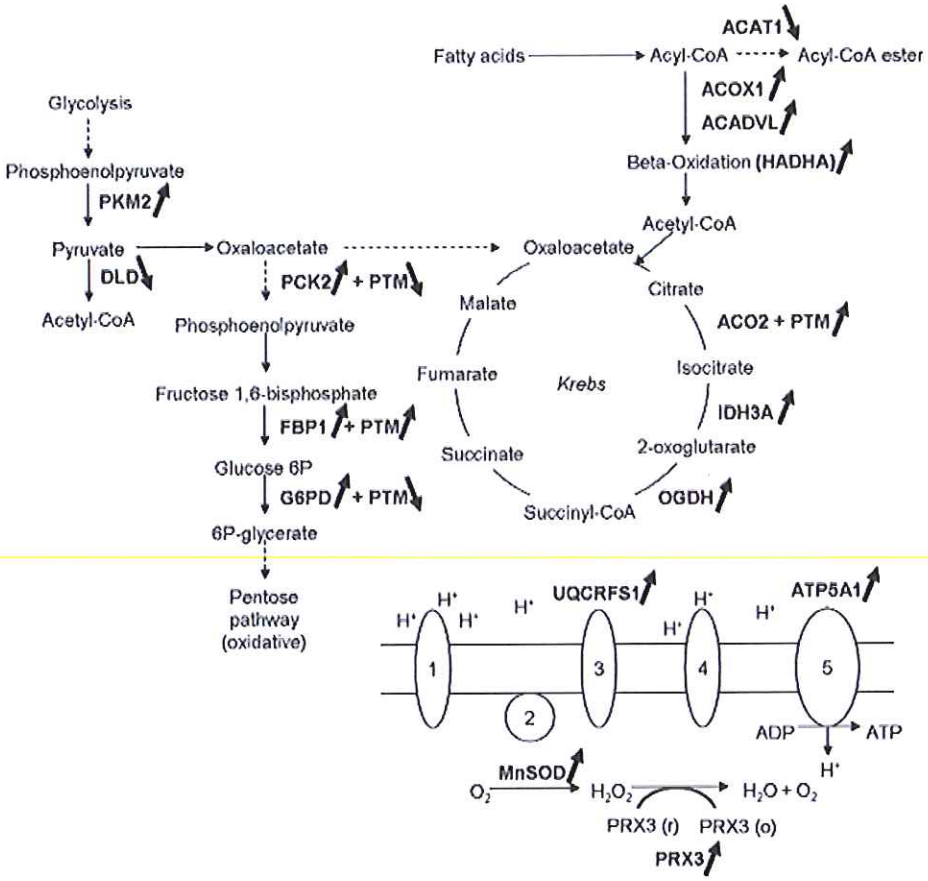


Figure 4. Schematic presentation of β-oxidation pathway and Krebs cycle, targeted by TX527 treatment in mDCs Scheme of the metabolism pathway including differentially expressed proteins identified in this study. For complete names of abbreviations see Supporting Information Table 2.

in mDCs together with a series of other anti-oxidant proteins, such as Prx1, enabling DCs to survive in a highly oxidant environment [17, 51].

Another major group of proteins affected by TX527 treatment is the protein biosynthesis/proteolysis group, which includes proteins involved in antigen processing and presentation. Many of the differentially expressed proteins identified from the 2-D DIGE analysis could be related to the MHCI and MHCII-linked pathways (Fig. 5). The alterations induced by TX527 treatment are opposite to what happens during the DC maturation process [17]. Proteins identified linked to the MHCI pathway were cytosol aminopeptidase (LAP3) and proteasome activator complex subunit 2 (PSME2), both down-regulated by the treatment with TX527. In addition, two endosomal proteases related to the MHCII, namely cathepsin D and S (CTSD and CTSS), were up-regulated. Overexpression of CTSD mRNA has been shown to be induced by either retinoic acid or $1,25(OH)_2D_3$ treatment in HL60 cells in a dose-dependent manner [52]. The higher expression of CTSS in DCs has been shown to decrease intracellular MHCII dimers as well as surface MHCII, reducing T-cell activation [53]. In addition to that, two subunits of the coatomer complex I (COPI), namely γ and δ, are targeted by TX527 in mDCs. The coatomer complexes are protein coats, which mediate vesicle budding, cycling on and off membranes. COPI primarily mediates vesicle trafficking from the Golgi to the ER and between Golgi cisternae [54]. After budding, vesicles are transported to their final destination where they will interact with the target membrane through a mechanism called tethering, which precedes membrane fusion mediated by soluble N-ethylmaleimide-sensitive factor attachment protein receptor (SNARE) proteins. In this venue, Rabs are a large family of GTPases that participate with SNAREs in vesicle targeting and membrane fusion [55]. Interestingly, one of the members of the Rab family, RabGDI, was found to be down-regulated (2.27-fold) by TX527 treatment in mDCs.

In conclusion, using a proteomic analysis based on 2-D DIGE and MALDI-TOF/TOF, we could identify several proteins targeted by the treatment with a vitamin D analogue, TX527, in human DCs. TX527 affects the proteome of human DCs in an integrated way, as shown by network analysis and affects mainly proteins involved in cytoskeleton, protein processing and cellular metabolism. In addition, we showed that these protein alterations were reflected in many features of the DCs, resulting in a distinct phenotypic state of these cells. Indeed, their morphology, surface phenotype, ability to migrate and to perform endocytosis of antigens were dramatically altered by

© 2009 WILEY-VCH Verlag GmbH & Co. KGaA, Weinheim

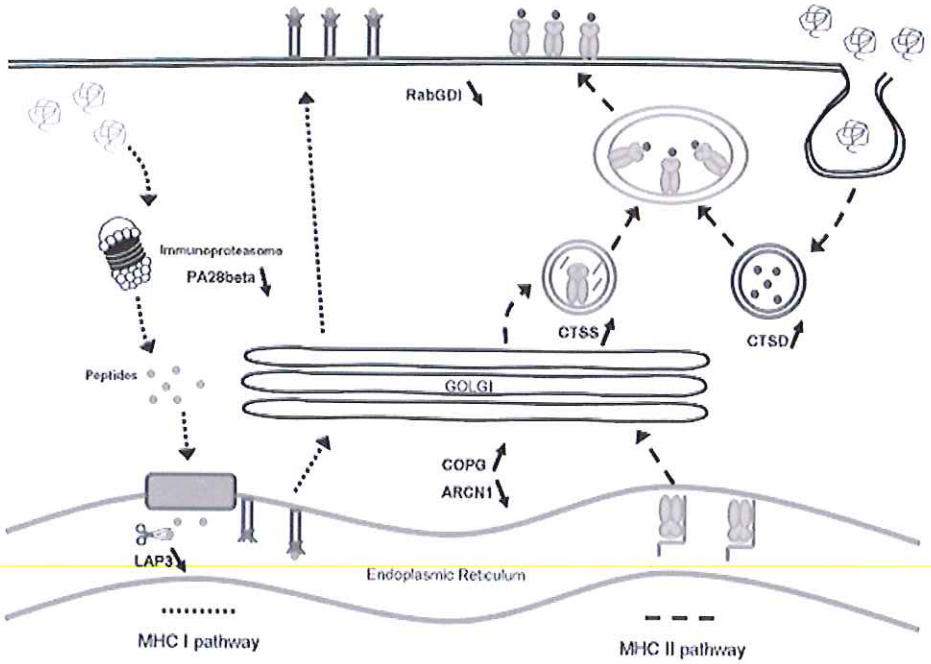


Figure 5. Schematic presentation of modulated antigen processing in TX527-treated humans DCs. In order to be presented by MHCI pathway, proteins are degraded by the proteasome in the cytosol. The resulting peptides are then trimmed by endoplasmic reticulum aminopeptidases to the correct length for MHCI antigen-presentation. For MHCII presentation, MHCII subunits assemble with the invariant chain (Ii) and this complex is exported to the Golgi compartment, later encountering acidified endosomal compartments. Here the Ii undergoes successive cleavages to obtain the class II-associated invariant chain peptide (CLIP) remaining on the MHCII peptide-binding site. CLIP is then changed for the antigenic peptide, which will be presented on the cell surface. Proteins differentially expressed and identified in this study are indicated in the figure. For complete names of abbreviations, see Supporting Information Table 2.

TX527 treatment. Taken together, the present findings reinforce the observations that analogues of vitamin D, such as TX527, fundamentally alter human DC phenotype and function, thus opening the possibilities of using these agents as immunomodulators in autoimmune conditions or in the prevention of graft destruction.

The technical experience of Karin Schildermans, Jos Depovere and Dirk Valckx is greatly appreciated. This work was supported by the Catholic University of Leuven (GOA 2004/10 and 2009/10), the Flemish Research Foundation (FWO G.0552.06 G.0649.08), the Belgium Program on Interuniversity Poles of Attraction initiated by the Belgian State (IUAP P5/17 and P6/40) and the Centre of Excellence SymBioSys (Research Council K.U.Leuven EF/05/007). G. B. F. is supported by a doctoral fellowship (Alban, no. E06D100904BR), E. V. E. by a post-doctoral fellowship (Juvenile Diabetes Research Foundation, JDRF3-2006-33), K.L. by a grant from Forsknigsrådet for Sundhed og Sygdom and C. M. by a clinical research fellowship (FWO). We further wish to thank the Villum Kann Rasmussen Foundation, the Simon Spies Foundation, the National Institute of Child Health and Development (NICHD) and the National Institute of Health (NIH) for financial support.

The authors have declared no conlict of interest.

5 References

[1] Deluca, H. F., Cantorna, M. T., Vitamin D: its role and uses in immunology. *FASEB J.* 2001, *15*, 2579–2585.

[2] Jones, G., Strugnell, S. A., DeLuca, H. F., Current understanding of the molecular actions of vitamin D. *Physiol. Rev.* 1998, *78*, 1193–1231.

[3] Hewison, M., Freeman, L., Hughes, S. V., Evans, K. N. *et al.*, Differential regulation of vitamin D receptor and its ligand in human monocyte-derived dendritic cells. *J. Immunol.* 2003, *170*, 5382–5390.

[4] Monkawa, T., Yoshida, T., Hayashi, M., Saruta, T., Identification of 25-hydroxyvitamin D3 1alpha-hydroxylase gene expression in macrophages. *Kidney Int.* 2000, *58*, 559–568.

[5] Overbergh, L., Decallonne, B., Valckx, D., Verstuyf, A. *et al.*, Identification and immune regulation of 25-hydroxyvitamin D-1-alpha-hydroxylase in murine macrophages. *Clin. Exp. Immunol.* 2000, *120*, 139–146.

[6] Penna, G., Adorini, L., 1 Alpha, 25-dihydroxyvitamin D3 inhibits differentiation, maturation, activation, and survival of dendritic cells leading to impaired alloreactive T cell activation. *J. Immunol.* 2000, *164*, 2405–2411.

[7] van Halteren, A. G., van Etten, E., de Jong, E. C., Bouillon, R. *et al.*, Redirection of human autoreactive T-cells upon interaction with dendritic cells modulated by TX527, an

© 2009 WILEY-VCH Verlag GmbH & Co. KGaA, Weinheim

analog of 1,25 dihydroxyvitamin D(3). *Diabetes* 2002, *51*, 2119–2125.

[8] Penna, G., Amuchastegui, S., Giarratana, N., Daniel, K. C. *et al.*, 1,25-Dihydroxyvitamin D3 selectively modulates tolerogenic properties in myeloid but not plasmacytoid dendritic cells. *J. Immunol.* 2007, *178*, 145–153.

[9] D'Ambrosio, D., Cippitelli, M., Cocciolo, M. G., Mazzeo, D. *et al.*, Inhibition of IL-12 production by 1,25-dihydroxyvitamin D3. Involvement of NF-kappaB downregulation in transcriptional repression of the p40 gene. *J. Clin. Invest.* 1998, *101*, 252–262.

[10] Piemonti, L., Monti, P., Sironi, M., Fraticelli, P. *et al.*, Vitamin D3 affects differentiation, maturation, and function of human monocyte-derived dendritic cells. *J. Immunol.* 2000, *164*, 4443–4451.

[11] De Clercq, P. J., Murad, I., Gao, L. J., Chen, Y. J. *et al.*, Biological activity and conformational analysis of C20 and C14 epimers of CD-ring modified trans-decalin 1alpha,25-dihydroxyvitamin D analogs. *J. Steroid Biochem. Mol. Biol.* 2004, *89–90*, 61–66.

[12] Verstuyf, A., Verlinden, L., Van Baelen, H., Sabbe, K. *et al.*, The biological activity of nonsteroidal vitamin D hormone analogs lacking both the C- and D-rings. *J. Bone Miner. Res.* 1998, *13*, 549–558.

[13] Verstuyf, A., Verlinden, L., van Etten, E., Shi, L. *et al.*, Biological activity of CD-ring modified 1alpha,25-dihydroxyvitamin D analogues: C-ring and five-membered D-ring analogues. *J. Bone Miner. Res.* 2000, *15*, 237–252.

[14] Verlinden, L., Verstuyf, A., Van Camp, M., Marcelis, S. *et al.*, Two novel 14-Epi-analogues of 1,25-dihydroxyvitamin D3 inhibit the growth of human breast cancer cells *in vitro* and *in vivo*. *Cancer Res.* 2000, *60*, 2673–2679.

[15] Van Etten, E., Decallonne, B., Verlinden, L., Verstuyf, A. *et al.*, Analogs of 1alpha,25-dihydroxyvitamin D3 as pluripotent immunomodulators. *J. Cell Biochem.* 2003, *88*, 223–226.

[16] D'Hertog, W., Overbergh, L., Lage, K., Ferreira, G. B. *et al.*, Proteomics analysis of cytokine-induced dysfunction and death in insulin-producing INS-1E cells: new insights into the pathways involved. *Mol. Cell. Proteomics* 2007, *6*, 2180–2199.

[17] Ferreira, G. B., Overbergh, L., van Etten, E., Lage, K. *et al.*, Protein-induced changes during the maturation process of human dendritic cells: 2-D DIGE approach. *Proteomics Clin. Appl.* 2008, *2*, 1349–1360.

[18] Bradford, M. M., A rapid and sensitive method for the quantitation of microgram quantities of protein utilizing the principle of protein–dye binding. *Anal. Biochem.* 1976, *72*, 248–254.

[19] Marouga, R., David, S., Hawkins, E., The development of the DIGE system: 2D fluorescence difference gel analysis technology. *Anal. Bioanal. Chem.* 2005, *382*, 669–678.

[20] Altschul, S. F., Madden, T. L., Schaffer, A. A., Zhang, J. *et al.*, Gapped BLAST and PSI-BLAST: a new generation of protein database search programs. *Nucleic Acids Res.* 1997, *25*, 3389–3402.

[21] Hinsby, A. M., Kiemer, L., Karlberg, E. O., Lage, K. *et al.*, A wiring of the human nucleolus. *Mol. Cell* 2006, *22*, 285–295.

[22] Lage, K., Karlberg, E. O., Storling, Z. M., Olason, P. I. *et al.*, A human phenome-interactome network of protein complexes implicated in genetic disorders. *Nat. Biotechnol.* 2007, *25*, 309–316.

[23] Bader, G. D., Betel, D., Hogue, C. W., BIND: the Biomolecular Interaction Network Database. *Nucleic Acids Res.* 2003, *31*, 248–250.

[24] Zanzoni, A., Montecchi-Palazzi, L., Quondam, M., Ausiello, G. *et al.*, MINT: a Molecular INTeraction database. *FEBS Lett.* 2002, *513*, 135–140.

[25] Hermjakob, H., Montecchi-Palazzi, L., Lewington, C., Mudali, S. *et al.*, IntAct: an open source molecular interaction database. *Nucleic Acids Res.* 2004, *32*, D452–D455.

[26] Kanehisa, M., Goto, S., Hattori, M., Aoki-Kinoshita, K. F. *et al.*, From genomics to chemical genomics: new developments in KEGG. *Nucleic Acids Res.* 2006, *34*, D354–D357.

[27] Joshi-Tope, G., Gillespie, M., Vastrik, I., D'Eustachio, P. *et al.*, Reactome: a knowledgebase of biological pathways. *Nucleic Acids Res.* 2005, *33*, D428–D432.

[28] Salwinski, L., Miller, C. S., Smith, A. J., Pettit, F. K. *et al.*, The Database of interacting proteins: 2004 update. *Nucleic Acids Res* 2004, *32*, D449–D451.

[29] Breitkreutz, B. J., Stark, C., Tyers, M., The GRID: the General Repository for Interaction Datasets. *Genome Biol* 2003, *4*, R23.

[30] O'Brien, K. P., Remm, M., Sonnhammer, E. L., Inparanoid: a comprehensive database of eukaryotic orthologs. *Nucleic Acids Res.* 2005, *33*, D476–D480.

[31] Lage, K., Hansen, N. T., Karlberg, E. O., Eklund, A. C. *et al.*, A large-scale analysis of tissue-specific pathology and gene expression of human disease genes and complexes. *Proc. Natl. Acad. Sci. USA* 2008, *105*, 20870–20875.

[32] Bergholdt, R., Storling, Z. M., Lage, K., Karlberg, E. O. *et al.*, Integrative analysis for finding genes and networks involved in diabetes and other complex diseases. *Genome Biol.* 2007, *8*, R253.

[33] Avramidou, A., Kroczek, C., Lang, C., Schuh, W. *et al.*, The novel adaptor protein Swiprosin-1 enhances BCR signals and contributes to BCR-induced apoptosis. *Cell Death Differ.* 2007, *14*, 1936–1947.

[34] Vuadens, F., Rufer, N., Kress, A., Corthesy, P. *et al.*, Identification of swiprosin 1 in human lymphocytes. *Proteomics* 2004, *4*, 2216–2220.

[35] van Halteren, A. G., Tysma, O. M., van Etten, E., Mathieu, C. *et al.*, 1alpha, 25-dihydroxyvitamin D3 or analogue treated dendritic cells modulate human autoreactive T cells via the selective induction of apoptosis. *J. Autoimmun.* 2004, *23*, 233–239.

[36] Banchereau, J., Briere, F., Caux, C., Davoust, J. *et al.*, Immunobiology of dendritic cells. *Annu. Rev. Immunol.* 2000, *18*, 767–811.

[37] Al-Alwan, M. M., Rowden, G., Lee, T. D., West, K. A., Fascin is involved in the antigen presentation activity of mature dendritic cells. *J. Immunol.* 2001, *166*, 338–345.

© 2009 WILEY-VCH Verlag GmbH & Co. KGaA, Weinheim

[38] Ross, R., Jonuleit, H., Bros, M., Ross, X. L. *et al.*, Expression of the actin-bundling protein fascin in cultured human dendritic cells correlates with dendritic morphology and cell differentiation. *J. Invest. Dermatol.* 2000, *115*, 658–663.

[39] Ross, R., Ross, X. L., Schwing, J., Langin, T. *et al.*, The actin-bundling protein fascin is involved in the formation of dendritic processes in maturing epidermal Langerhans cells. *J. Immunol.* 1998, *160*, 3776–3782.

[40] Chen, H., Bernstein, B. W., Bamburg, J. R., Regulating actin-filament dynamics *in vivo*. *Trends Biochem. Sci.* 2000, *25*, 19–23.

[41] Nagaoka, R., Abe, H., Kusano, K., Obinata, T., Concentration of cofilin, a small actin-binding protein, at the cleavage furrow during cytokinesis. *Cell Motil. Cytoskeleton.* 1995, *30*, 1–7.

[42] Shutt, D. C., Daniels, K. J., Carolan, E. J., Hill, A. C. *et al.*, Changes in the motility, morphology, and F-actin architecture of human dendritic cells in an *in vitro* model of dendritic cell development. *Cell Motil. Cytoskeleton* 2000, *46*, 200–221.

[43] Verdijk, P., van Veelen, P. A., de Ru, A. H., Hensbergen, P. J. *et al.*, Morphological changes during dendritic cell maturation correlate with cofilin activation and translocation to the cell membrane. *Eur. J. Immunol.* 2004, *34*, 156–164.

[44] Mullins, R. D., Heuser, J. A., Pollard, T. D., The interaction of Arp2/3 complex with actin: nucleation, high affinity pointed end capping, and formation of branching networks of filaments. *Proc. Natl. Acad. Sci. USA* 1998, *95*, 6181–6186.

[45] Fujibuchi, T., Abe, Y., Takeuchi, T., Imai, Y. *et al.*, AIP1/WDR1 supports mitotic cell rounding. *Biochem. Biophys. Res. Commun.* 2005, *327*, 268–275.

[46] DerMardirossian, C., Bokoch, G. M., GDIs: central regulatory molecules in Rho GTPase activation. *Trends Cell Biol.* 2005, *15*, 356–363.

[47] Pereira, S. R., Faca, V. M., Gomes, G. G., Chammas, R. *et al.*, Changes in the proteomic profile during differentiation and maturation of human monocyte-derived dendritic cells stimulated with granulocyte macrophage colony stimulating factor/interleukin-4 and lipopolysaccharide. *Proteomics* 2005, *5*, 1186–1198.

[48] Gauzzi, M. C., Purificato, C., Donato, K., Jin, Y. *et al.*, Suppressive effect of 1alpha,25-dihydroxyvitamin D3 on type I IFN-mediated monocyte differentiation into dendritic cells: impairment of functional activities and chemotaxis. *J. Immunol.* 2005, *174*, 270–276.

[49] Szatmari, I., Torocsik, D., Agostini, M., Nagy, T. *et al.*, PPARgamma regulates the function of human dendritic cells primarily by altering lipid metabolism. *Blood* 2007, *110*, 3271–3280.

[50] Dai, X., Sayama, K., Shirakata, Y., Tokumaru, S. *et al.*, PPAR gamma is an important transcription factor in 1 alpha, 25-dihydroxyvitamin D3-induced involucrin expression. *J. Dermatol. Sci.* 2008, *50*, 53–60.

[51] Rivollier, A., Perrin-Cocon, L., Luche, S., Diemer, H. *et al.*, High expression of antioxidant proteins in dendritic cells: possible implications in atherosclerosis. *Mol. Cell. Proteomics* 2006, *5*, 726–736.

[52] Atkins, K. B., Troen, B. R., Regulation of cathepsin D gene expression in HL-60 cells by retinoic acid and calcitriol. *Cell Growth Differ.* 1995, *6*, 871–877.

[53] Kitamura, H., Kamon, H., Sawa, S., Park, S. J. *et al.*, IL-6-STAT3 controls intracellular MHC class II alphabeta dimer level through cathepsin S activity in dendritic cells. *Immunity* 2005, *23*, 491–502.

[54] Waters, M. G., Serafini, T., Rothman, J. E., 'Coatomer': a cytosolic protein complex containing subunits of non-clathrin-coated Golgi transport vesicles. *Nature* 1991, *349*, 248–251.

[55] Zerial, M., McBride, H., Rab proteins as membrane organizers. *Nat. Rev. Mol. Cell. Biol.* 2001, *2*, 107–117.

© 2009 WILEY-VCH Verlag GmbH & Co. KGaA, Weinheim